

Tutorial — time conversion of depth migrated data: part II, TTI preSDM

Ian F. Jones^{1*}

Abstract

Contemporary depth imaging projects often require final pre-Stack Depth-Migrations (preSDM) to be converted to time for comparison to vintage pre-Stack Time-Migrations (preSTM), or to facilitate conversion to ‘geological’ depth through calibration to well and check-shot data. Here, I consider the situation of having performed an anisotropic Tilted Transverse Isotropy (TTI) preSDM and wanting to convert it to time via vertical stretch in order to compare it, say, to an anisotropic preSTM.

Such a comparison is inherently invalid, as time-migration will explicitly treat any anisotropy as if it were Vertical Transverse Isotropy (VTI), and, in addition, the lateral positioning error inherent in preSTM will render such comparisons questionable on steeply dipping structures.

I show here that the most appropriate type of ‘velocity’ to use for conversion to time of TTI preSDM reflection events should be the vertical component of the phase velocity. Conversely, if we are considering point-to-point measurements, such as the direct arrival travel time, a down-hole or check-shot measurement, then the group velocity should be used, as it is with this speed that energy travels. In addition, subsequent depth conversion of any time product for interpretational purposes would best be accomplished using a velocity calibrated to well check-shots.

Introduction

In an earlier tutorial on time conversion of isotropically depth migrated data (Jones 2009), I considered the case of a preSDM being converted to time via vertical stretch, and assessed the merits of converting a depth migrated image to time with either a smooth or a highly detailed velocity model. When we have a depth migrated image, the associated velocity field is in general not smooth. It is this lack of smoothness, especially in the lateral sense, which was addressed in my 2009 tutorial. There, it was demonstrated that the best route for conversion depended on the intended objective, but, usually, a smooth velocity model would be best if pre-stack post-processing, auto-picking, or direct comparison to a preSTM, was the objective.

In this update on the topic, I consider the situation where we have performed a TTI preSDM and want to compare it to say an anisotropic preSTM, which, by the nature of time-migration, will inherently treat any anisotropy as if it were VTI. In addition, for anisotropic media the situation becomes more complex, as we have to consider both the group and phase velocities of the wavefield.

The two issues which arise in such a comparison of a preSTM and time-converted TTI preSDM relate primarily to 1) the appropriate type of ‘velocity’ to use in the vertical conversion (i.e. should we use the migration TTI polar velocity, or the vertical component of group velocity, or the vertical component of phase

velocity?); 2) the inherent lateral positioning difference between a time and a depth migration for steeply dipping events.

There is also the issue of what kind of measurements we want to compare: for example, if we are comparing images, then it will be shown that it is the vertical component of the phase velocity that should be used. Recall that images are formed by the superposition of wavefronts arriving with stationary phase, which when considered as locally plane waves, will travel at the phase velocity. However, if we are considering point-to-point measurements, such as the direct arrival travel time, a down-hole or check shot measurement, then the group velocity should be used, as it is with this speed that energy travels on a point-to-point travel path.

In addition, regardless of whether we are dealing with a depth migration that has been converted to time, or a time-migration image itself, we also have the issue of how to convert a time image to geological depth ready for interpretation (usually achieved by comparing to check-shot data or by tying calibrated reflectors in time to well markers in depth).

Also, it should be noted that the discussion of converting a preSDM to the time domain is subtly different than that of converting a preSTM to depth (the process of ‘depthing’; Al-Chalabi, 1974; 1994; 1997; Al-Chalabi and Rosenkranz, 2002; Al-Chalabi, 2014; Armstrong, 2001; Armstrong et al., 2001; Bartel et al., 2006; Cameron et al., 2008; Grechka et al., 1999; Iversen and Tygel, 2008) as the depthing procedure is internally consistent in

¹ ION

* Corresponding author, E-mail: ian.jones@iongeo.com

DOI: 10.3997/1365-2397.2019039

θ : wavefront angle from the polar axis
 φ : ray angle from the polar axis

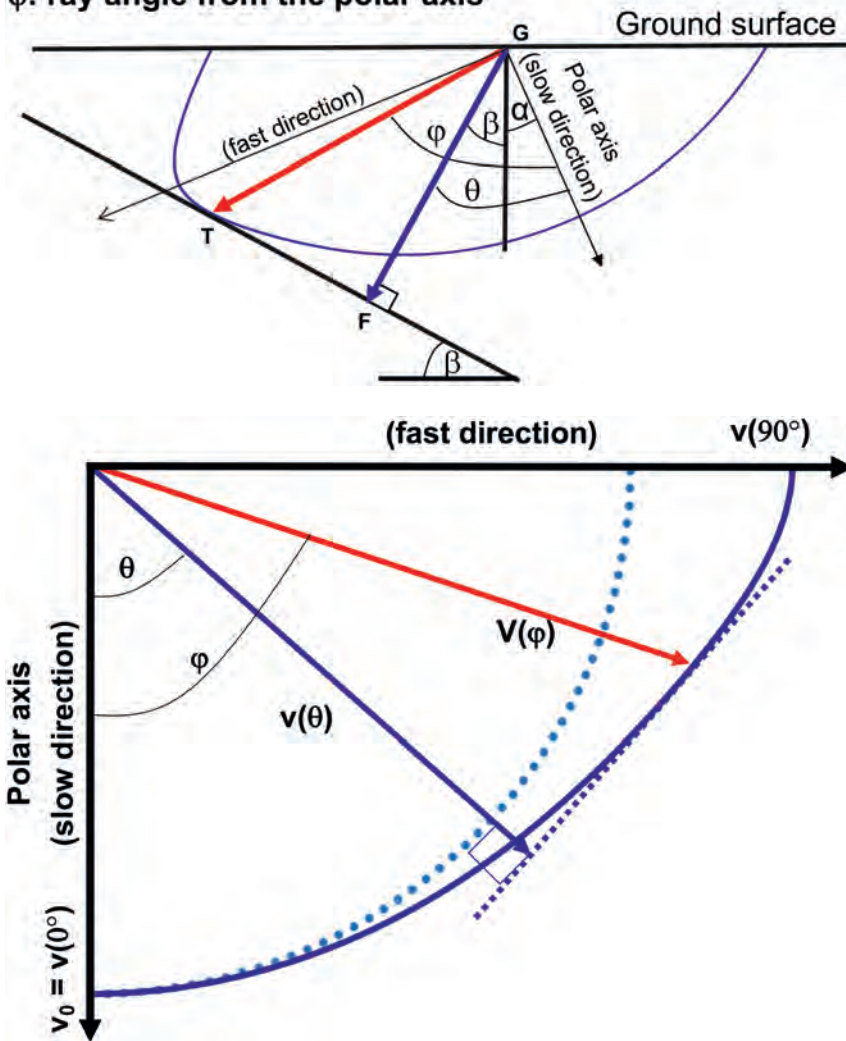


Figure 1 A wavefront that reflects back from the dipping reflector represents a constant phase event (plane wave), and travels in the direction GF at the **phase velocity**, indicated by the blue arrow (for the 'normal reflection' plane wave at reflector dip β). Energy is transmitted along the raypath in direction GT at the **group velocity**, indicated by the red arrow.

Figure 2 When the medium is isotropic: the wavefront is a semi-circle (purple circular dotted curve in the figure), $\theta = \varphi$, and phase velocity = group velocity. Otherwise the wavefront looks like a squashed ellipse (solid blue curve) of which the fast and slow speeds are related by $v_{fast} = v_{slow} * (1 + \epsilon)$. The blue dotted straight line represents the tangent to the wavefront in the ray direction φ . The normal to this tangent meets the origin at the phase angle θ .

that it uses techniques that do not address the velocity dependence of lateral changes in structural positioning.

Health warning!

By way of a preamble, before dealing with the main topic itself, it is worth reminding ourselves that a time migration has no physical meaning. The underlying assumption upon which time-migration is based, is that over the width of the migration operator the Earth has no lateral parameter change: this assumption is usually unfounded. Furthermore, if we have a reasonable depth image, wherein lateral parameter change has been sensibly addressed, then it makes little sense to try to compare it to a time migration for the purposes of positioning verification, as there will be significant lateral positioning differences which cannot be reconciled via a simple vertical stretch from depth to time. At best, we might be able to make a localized comparison on a single structural element, but drawing conclusions of comparisons between diverse structures will be very misleading. However, from a seismic contractor's point of view, we are almost always required to perform time conversion of depth migrated data, usually for the purposes of post-processing with time domain algorithms (for example, suppression of residual multiples using

a Radon filter). Also, interpreters often want to compare a depth migrated result to a vintage time product in the same domain and this tutorial addresses the lesser evil of performing such a conversion with the most appropriate velocity.

In addition, for the purposes of simplicity, I am assuming here that we are comparing ray-based migration results, such as those produced via Kirchhoff or beam migration. Dealing with wave-field extrapolation images would introduce more confusion, as it would necessitate discussion of the limits of the high frequency approximation versus accommodating energy within the Fresnel zone. Further discussion on such difference, and also the shortcoming of time migration in general, can be found in Hubral (1977) and Black and Brzostowski (1994).

Anisotropic wave propagation in a transversely isotropic (TI) medium

Energy travels from the source carried by the wavefront, in a direction specified by a ray, at the group velocity. However, a reflector gives rise to a plane-wave-like coherent reflection formed by superposition of wavefronts that travels back to the surface at an apparent velocity referred to as the phase velocity. For normal incidence, this reflection comes back from the reflec-

tor at a right angle (Alkhalifah and Tsvankin, 1995; Alkhalifah, 1997).

Consider a compressional (P-wave) wavefront propagating from surface point G in a transversely isotropic medium with TTI polar axis tilt angle α (Figure 1). If this wavefront encounters a reflector dipping at angle β (at point T), then the tangent to the wavefront at point T would be parallel to the reflector. If you think of the wavefront as being composed of plane waves, then for a receiver also at point G, the ray will reflect back from T to point G (this is the zero offset case, but here we do not have normal incidence at zero-offset as the medium is TTI). The speed in this direction (G to T) is the **group velocity** and this is the speed at which energy travelled along the raypath in the medium: this raypath is at angle φ to the polar axis. However, the normal to the reflector (at point F) will be at angle θ to the polar axis (and angle β to the vertical), and a wavefront that reflects back from the dipping reflector represents a constant phase (plane wave) and travels in the direction FG at the **phase velocity** for direction θ relative to the polar axis. So in a TTI medium, as the phase and group angles are different, so the phase and group velocities will be different (Berryman, 1979; Thomsen, 2002; Grechka, 2009).

Definition of the phase angle θ and the group angle φ

Energy travels in the ‘ray’ direction at the group velocity, $\mathbf{V}(\varphi)$, but the normal to the wavefront travels at the phase velocity, $\mathbf{v}(\theta)$ (as indicated in Figure 2). However, it is constructive interference between wavefronts that builds the image, so the phase velocity is what governs the positions of reflectors in the image. It is common practice that the parameters we provide to the TTI imaging algorithm are the phase velocity in the direction of the polar axis: v_0 as well as Thomsen’s parameters δ , ϵ , and the structural dip information dipX, dipY (Thomsen 1986; 2002). (N.B. along the polar axis and normal to it, i.e. the slow and fast directions, phase and group velocities are the same as $\theta=\varphi=0^\circ$ or $\theta=\varphi=90^\circ$ as the wavefront is normal to the ray in these directions).

Ray tracing proceeds using the ray angle φ (group velocity direction). However, for Thomsen’s formulation of weak polar

anisotropy, the anisotropy is characterized using the phase velocity and phase angle θ , thus algorithmic complexity is involved in moving from the user supplied parameters to the actual tracing of rays (Wang 2014). Although energy moves along the ray direction, when the raypath encounters an interface and refracts (in accordance with Snell’s law), the refraction must employ the phase angle and phase velocities, as they pertain to the wavefront normal, i.e. are representative of the hypothetical underlying plane waves (e.g. Sadri and Riahi, 2010).

The change in phase velocity as a function of direction (with respect to the polar axis) is given by Thomsen 1986:

$$v(\theta) \approx v_0 \left(1 + \delta \cos^2(\theta) \sin^2(\theta) + \epsilon \sin^4(\theta) \right) \quad (1)$$

Where, as denoted in Figure 2, v_0 is the velocity in the direction of the anisotropy polar axis, $\mathbf{v}(\theta)$ is the phase velocity corresponding to the direction of the phase angle θ , and $\mathbf{V}(\varphi)$ is the group velocity, corresponding to the group velocity angle φ .

The relationship between the group velocity, $\mathbf{V}(\varphi)$, and the phase velocity, $\mathbf{v}(\theta)$ is given by (Berryman 1979):

$$V(\varphi(\theta))^2 = v(\theta)^2 + \left(\frac{\partial v}{\partial \theta} \right)^2 \quad (2)$$

So by using (1) to evaluate the partial derivative of v with respect to θ we can obtain $\mathbf{V}(\varphi)$.

$$V(\varphi(\theta))^2 = v(\theta)^2 + v_0^2 \left(2\delta \cos(\theta) \sin(\theta) + 4(\epsilon - \delta) \cos(\theta) \sin^3(\theta) \right)^2 \quad (3)$$

Whereas the group and phase angles themselves are related by:

$$\tan(\varphi) = \tan(\theta) \left(1 + 2\delta + 4(\epsilon - \delta) \sin^2(\theta) \right) \quad (4)$$

However, if we assume that the terms in $\cos(\theta)$ and $\sin(\theta)$ in equation (3) are small, we can make the weak anisotropic approximation proposed by Thomsen (1986) and use:

$$V(\varphi(\theta)) = v(\theta) \quad (5)$$

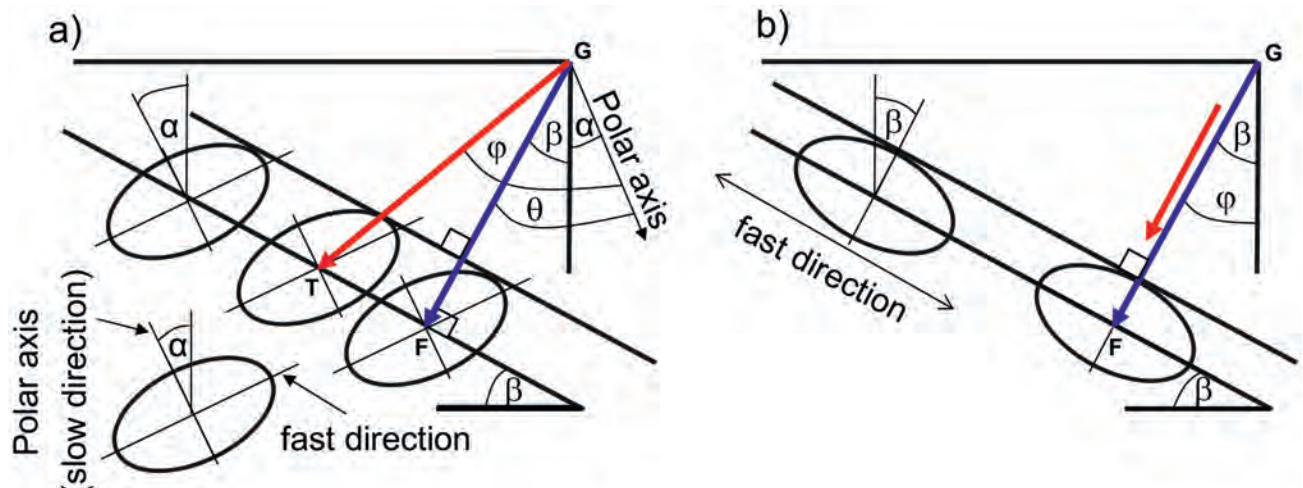


Figure 3 a) Reflected wavefront in the case with general polar axis. θ = wavefront angle from the polar axis, φ = ray angle from the polar axis, v_0 is the phase velocity in the direction of the polar axis (the slow direction). Thomsen’s parameters δ , ϵ are specified with respect to the polar axis. b) In this case we have assumed that $\alpha = \beta$ i.e. the polar symmetry axis is the same as the bedding axis, i.e. structural axis TTI. Here, for the direction of the zero-offset ray path, GT, the ray and phase directions are the same because the polar axis is conformable with the structural axis.

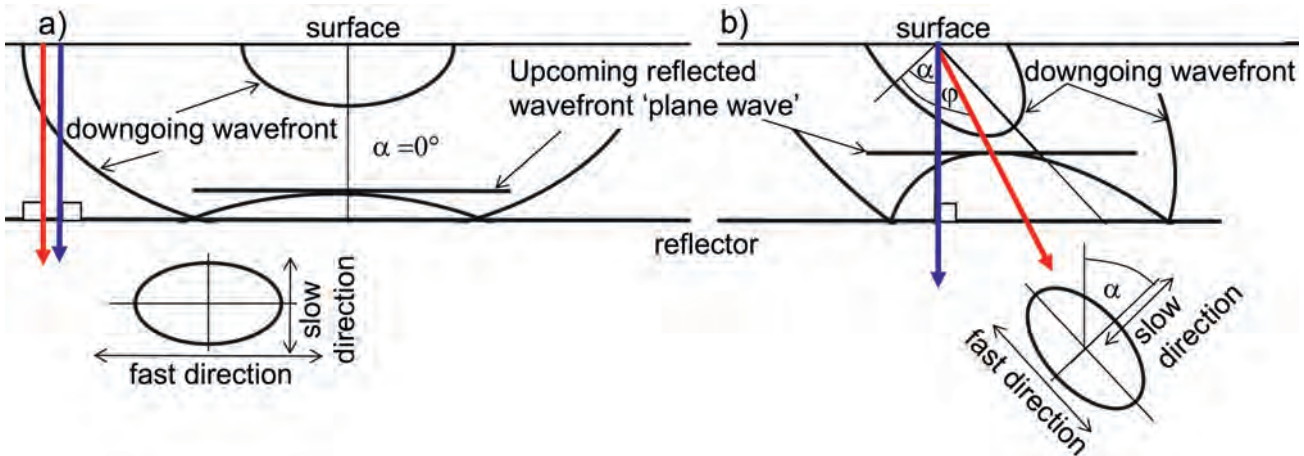


Figure 4 a) Scenario 1; flat layers with a vertical polar axis. b) Scenario 2, flat layers with a tilted polar axis. Blue arrow denotes phase velocity direction, red arrow denotes group velocity direction.

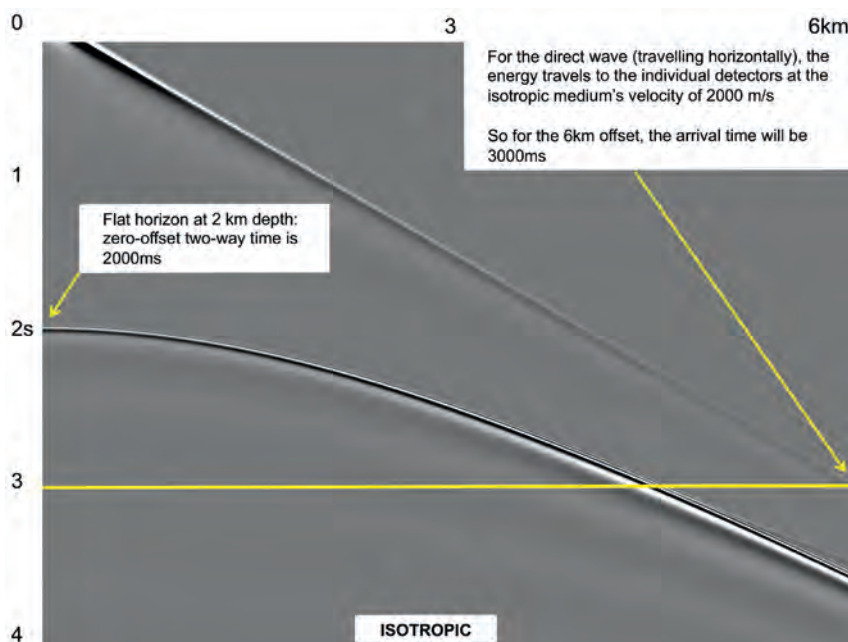


Figure 5 Isotropic gather. Zero-offset two-way time is 2 s. For the direct wave (travelling horizontally).

Anisotropic wave propagation in a transversely isotropic (TI) medium

A wavefront that reflects from a dipping reflector represents a constant phase (plane wave) and travels in the direction FG (in Figure 1) at the **phase velocity** (for the plane wave at reflector dip β). If we take α as the anisotropy polar axis tilt angle, then, if $\alpha = 0^\circ$ we have vertical transverse isotropy VTI, and if $\alpha \neq 0^\circ$ then we have tilted transverse isotropy TTI. Furthermore, if we make the assumption that $\alpha = \beta$, then we have structural axis TTI wherein the polar axis is perpendicular to the bedding planes: for pragmatic reasons industrial applications of anisotropic imaging usually make this assumption. If $\alpha = 90^\circ$ we have ‘fracture related’ horizontal transverse isotropy HTI (Uren et al., 1990; Tsvankin and Thomsen, 1994; Alkhalifah and Tsvankin, 1995; Tsvankin, 1997; Vernik and Liu, 1997).

Figure 3a shows the situation of the most general TI case, and Figure 3b shows the case where the polar axis is taken to be the same as the structural axis. This is frequently assumed to be the case, although it is not necessarily a valid assumption (see for example Jones and Davison, 2014).

Time versus depth imaging

Hitherto, I have discussed how wavefronts propagate in anisotropic media. Let’s now consider what we assume when we build an image by migrating the recorded data with either a time or a depth migration algorithm. The most important difference between a time and a depth migration scheme is that a depth scheme tries to accommodate the effects on wave propagation of lateral parameter variation, whereas time migration makes the gross simplifying assumption that all parameters are locally laterally invariant on a scale-length equal to the migration operator width – which is many kilometres (e.g. Robein 2003, 2010, Jones 2010, 2015). This difference manifests itself primarily in the lateral positioning error on dipping structures in a time migrated image. These positioning errors are more pronounced once we incorporate anisotropy within the migration scheme (Verwest, 1989; Alkhalifah and Larner, 1994; Vestrum et al., 1999; Jones et al., 2003; Bakulin et al., 2010).

This observation underpins the futility of trying to meaningfully compare a vertically stretched (time-converted) depth migrated image with a time migrated image, as the requisite

conversion velocity would need to change laterally and vertically in a bizarre manner. However, given that we are often obliged to make such a comparison, we can at least strive to do so in the more sensible and consistent manner.

Converting a TTI preSDM to time

To some extent, how we do this depends on what we hope to achieve. For example, as considered in the first time-conversion tutorial which dealt with the isotropic case (Jones, 2009), if we intend to apply a Radon filter say for noise or multiple suppression, then almost any meaningful but smooth velocity function will suffice (as long as we back it off later).

However, if we wish to compare the TTI preSDM with a previously created preSTM then things are more complex. The reflection energy appears in the seismic data at the location where

the wavefronts constructively interfere: at a position reached with the phase velocity (and more usually, due to our assumptions, at the phase velocity in a direction equal to the dip of the reflector being imaged). If the subsurface was indeed anisotropic with a tilted axis, then we need to consider how a preSTM dealt with this.

Recall that preSTM assumes symmetric operators, corresponding to a vertical axis of symmetry; hence preSTM is assuming that in the vertical propagation direction the group velocity and phase velocity are identical. So in practice we will have two scenarios depending on whether the subsurface actually had a tilted polar axis or a vertical axis.

The cartoon in Figure 4 shows the downgoing wavefront and upcoming plane wave reflection for these two scenarios, and Figures 5, 6, and 7 show acoustically modelled shot gathers for the isotropic and two anisotropic cases.

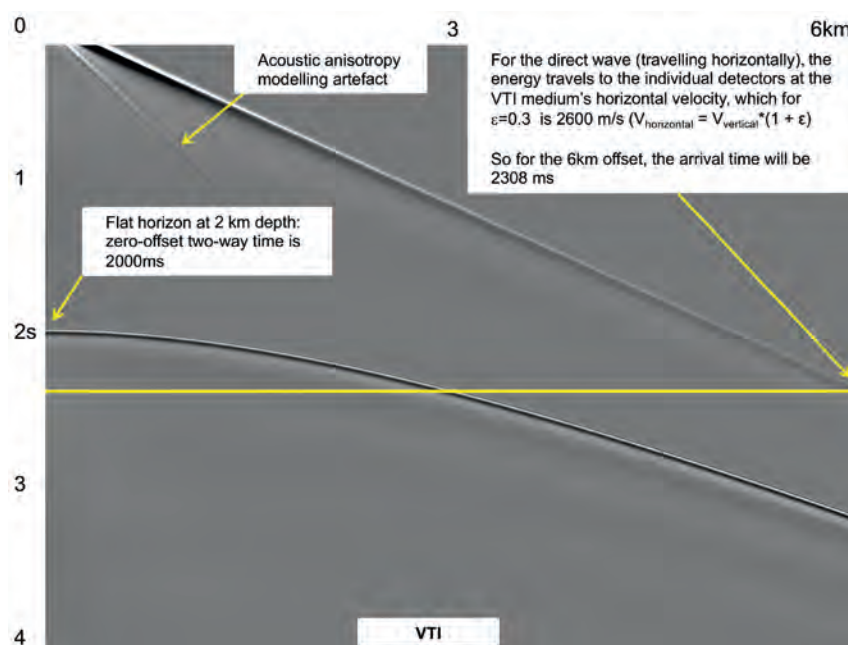


Figure 6 VTI Anisotropic gather— $\delta = 10\%$, $\epsilon = 30\%$, reflector dip = 0° , polar dip = 0° , zero-offset two-way time is 2 s.

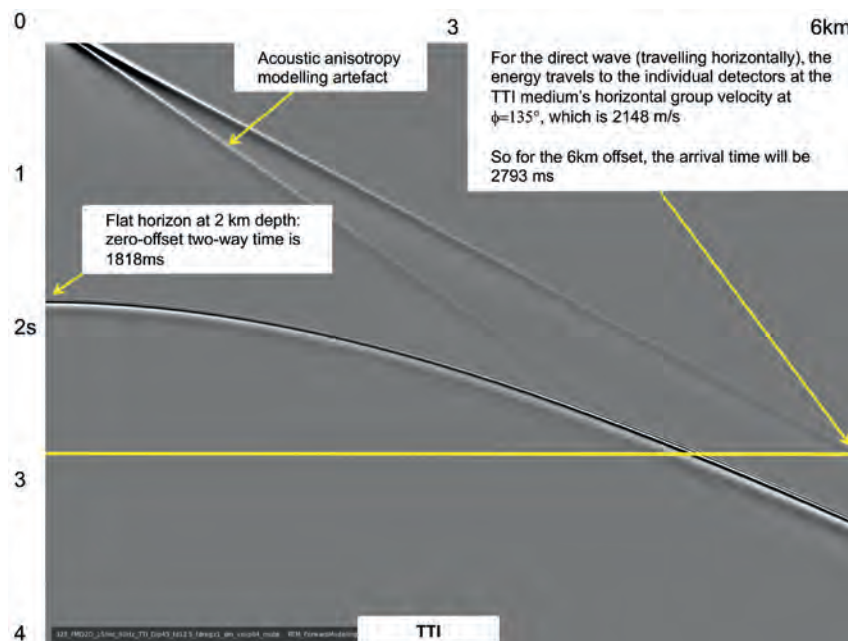


Figure 7 TTI Anisotropic gather— $\delta = 10\%$, $\epsilon = 30\%$, reflector dip = 0° , polar dip = 45° , zero-offset two-way time is 1.818 s.

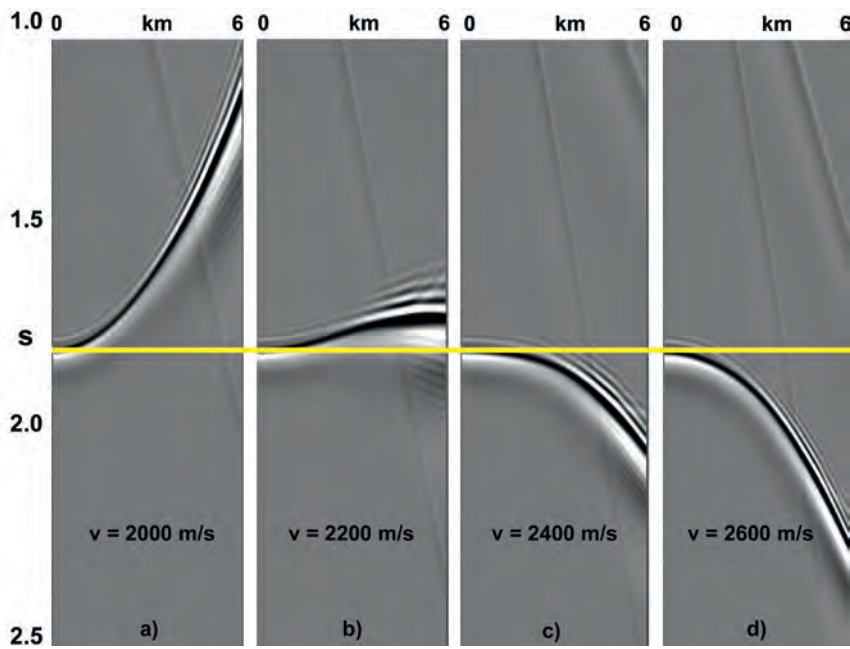


Figure 8 TTI anisotropic data after isotropic preSTM - gathers after constant velocity migration with a) $v=2000$ m/s, b) $v=2200$ m/s, c) $v=2400$ m/s, d) $v=2600$ m/s. The flattest gather is obtained with migration using the V_{nmo} velocity of between 2200 m/s - 2400 m/s. The horizontal line is positioned at $t=1.8$ s.

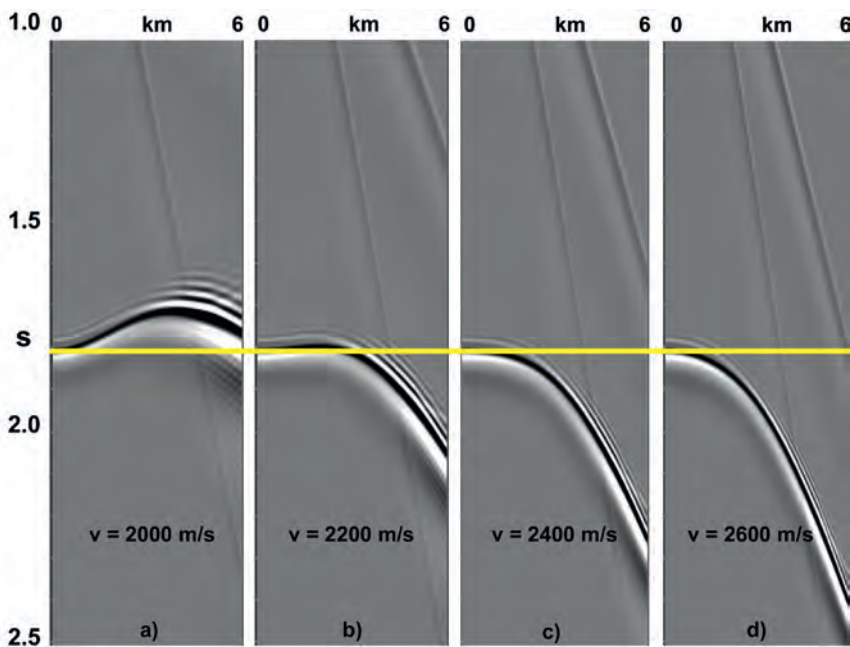


Figure 9 TTI anisotropic data after VTI preSTM - gathers after constant velocity migration with a) $v = 2000$ m/s, b) $v = 2200$ m/s, c) $v = 2400$ m/s, d) $v = 2600$ m/s. The flattest gather is obtained with migration using the V_{nmo} velocity of between 2200 m/s-2400 m/s. The horizontal line is positioned at $t = 1.8$ s.

Scenario 1: If the subsurface indeed has a vertical polar axis (VTI): Figure 4a.

The polar axis is the reference direction for the **phase velocity**. For a flat reflector with a vertical polar axis, a zero offset raypath propagates vertically with **group velocity = phase velocity** = v_0 . For a reflector at 2 km depth, the reflection event we see is formed from coherent phase interference: given a polar velocity of 2000 m/s, the zero offset arrival time will be 2.0 s. In this case there is no problem as there is only one ‘vertical’ velocity and no lateral positioning distortion would be expected.

Scenario 2: if the subsurface has a tilted polar axis (TTI): Figure 4b.

Now consider the situation where we might have transversely isotropic shale beds, tilted at 45° , sitting on top of a

flat reflector (e.g. Vernik and Liu, 1997; Vestrum et al., 1999). With a structurally conformable polar axis tilted at $\alpha = 45^\circ$, and $v_0 = 2000$ m/s, $\epsilon = 30\%$, $\delta = 10\%$, a zero offset raypath ($\theta = 45^\circ$) for a flat reflector propagates with phase velocity given by equation (1), which yields $v_{(45)} = 2200$ m/s.

So for the flat reflector at 2 km depth, the zero offset arrival time will be 1.818 s. (In this case, the group angle $\varphi \approx 58^\circ$ and $V_{group} \approx 2280$ m/s). However, velocity analysis for stacking and time migration will yield a best fit approximation to the complex anisotropic moveout yielding $V_{nmo} \approx 2400$ m/s, and a purely hyperbolic fit over a 6 km offset range of $V_{stacking} \approx 2800$ m/s. In Figure 4b, the case of a flat reflector is described in order to simplify the diagram. However, the same relationship between the group and phase velocities would apply to the case of a dipping reflector.

For a medium which is isotropic, the zero offset two-way travel time with $v_0 = 2000$ m/s, is 2 s (Figure 5). The direct wave, travelling horizontally with the same speed reaches the far offset for a 6 km cable, at one-way travel time 3 s.

For anisotropic scenario 1, everything is consistent so there is no real problem. This corresponds to the synthetic data shown in Figure 6, which was created with a vertical polar axis (i.e. $\alpha = 0^\circ$). Here the zero offset time is the same as for an isotropic material (Figure 5) as this is the slow-speed direction, but the far offset travel times in the VTI medium will be decreased by the higher horizontal velocity component (2600 m/s). Hence the VTI far offset arrival (as well as the direct wave) arrive at a lesser time than in the isotropic medium. In both figures 6 and 7, there appears to be a linear event labelled as being an acoustic anisotropy modelling artefact: given that anisotropy is a purely elastic phenomena, when we attempt to model it with an acoustic wave propagator, a pseudo-elastic ‘ghost’ artefact is created (appearing where the elastic shear event would have been; eg. Alkhalifah, 2000; Bale, 2007)

For scenario 2, it is more complex. Let us assume that the TTI preSDM was ‘correct’, and imaged the flat reflector at its true depth of 2 km in a subsurface with polar axis tilt $\alpha = 45^\circ$, $\epsilon = 30\%$, $\delta = 10\%$, with anisotropic migration velocity $v_0 = 2000$ m/s (which pertains to the ‘slow’ direction), and we now want the vertical time corresponding to this depth to match what the preSTM gave in its migrated image. As seen in Figure 7, in the TTI medium, the zero offset time is 1.818 s, as the vertical wave travels with a velocity higher than the polar direction velocity.

The preSTM incorrectly assumed that the polar axis was vertical, i.e., group velocity = phase velocity for a zero-offset vertical travel path to the flat reflector. The velocity we estimate from the data for time migration is derived from best-fit hyperbolic or 4th order fitting, and is likely to be higher than 2200 m/s (seen by the near offsets). However, the zero-offset time in the preSTM gathers will still be 1.818 s, but the gathers will have some RMO after migration with the derived velocity, so the corresponding image will be a bit distorted.

To vertically convert the TTI depth imaged horizon at $z = 2$ km to a two-way time of 1.818 s (in order to match the preSTM), we need a vertical conversion velocity of 2200 m/s. This corresponds to the vertical component of the depth migration’s reference phase velocity, as obtained from equation 1, with $\theta = 45^\circ$ (as the vertical is at 45° to the polar axis).

Taking the data for the flat lying horizon underlying a TTI medium with 45° polar axis, as shown in Figure 7, and per-

forming isotropic time migration, we get the resulting Common Reflection-Point (CPR) gathers shown in Figure 8. To assess the effect of migration velocity, the data were migrated with a range of constant velocities, namely 2000, 2200, 2400, 2600 m/s. From visual inspection the gathers appear flattest (using a 2nd-order moveout equation) for a migration velocity of between 2200 m/s-2400 m/s. This value is also obtained from hyperbolic velocity analysis over the first 2 km of offsets of the (unmigrated) input data. In other words, we commit an error by fitting a hyperbolic trajectory to the tilted axis TTI moveout behaviour, falsely treating it as if it were data from an isotropic or VTI medium. The theoretical expression for V_{nmo} for a flat reflector underlying a TTI medium with these parameters would actually predict $V_{\text{nmo}} = 2600$ m/s (Tsvankin, 1997, equation B10). However, as expected, the flat event still appears at arrival time $t = 1.818$ s, hence, in order to convert the correct TTI preSDM image at 2 km depth to match it, we indeed require a vertical conversion velocity equal to the vertical component of the phase velocity (i.e. 2200 m/s). This test was repeated for VTI preSTM (using the correct TTI anisotropy parameters, which for VTI will be suboptimal) and is shown in Figure 9.

Well-ties and flat features on steeply dipping parallel beds.

If there were steeply dipping beds then the situation is much more confusing. The preSTM will have a significant lateral positioning error, composed of a lateral shift due to the general assumptions of time migration (even for isotropic media) plus a component of ‘side-slip’ resulting from mistreating the anisotropy (e.g. Vestrum et al., 1999) and this can falsely appear to be a vertical time shift as well. This is especially true if we have many parallel dipping layers, as it becomes very difficult to identify if a given reflector seismic event’s ‘wobble’ has moved vertically or laterally.

Consider for example a situation which is common offshore Nigeria, where we have steeply dipping parallel beds, all looking very similar (e.g. Sugrue et al., 2011). Figure 10a shows a cartoon representing both the underlying geology with the anisotropy polar axis conformable with the bedding (structural TTI) and a TTI preSDM image. We will assume that the blue dot on the blue horizon represents the location of a flat oil-water contact abutting the dipping blue horizon. In the correct TTI preSDM the dot is in its correct geological location (correct depth z_c , and lateral location x). Now consider what a time migration will do with the input data. In the TTI preSTM, the fast direction is at 45° dip, and

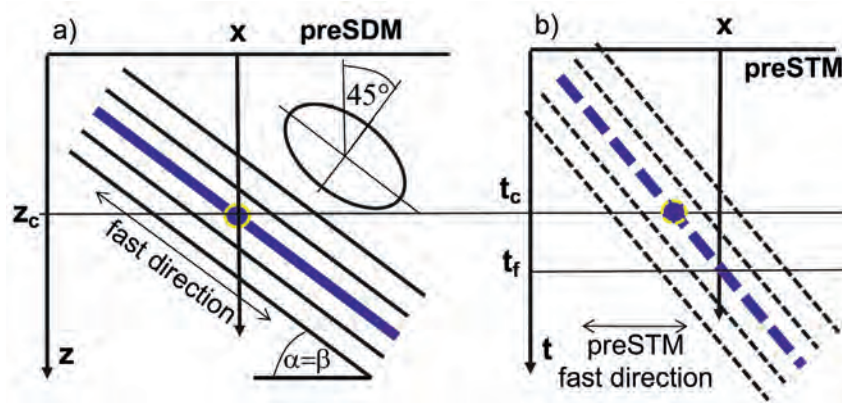


Figure 10 The lateral shift of the time migration comprises an anisotropy component plus a preSTM versus preSDM component. a) Correct preSDM image, representing geology, with marker location (z_c , x). b) PreSTM, with marker image at time t_c , but with expected lateral mispositioning.

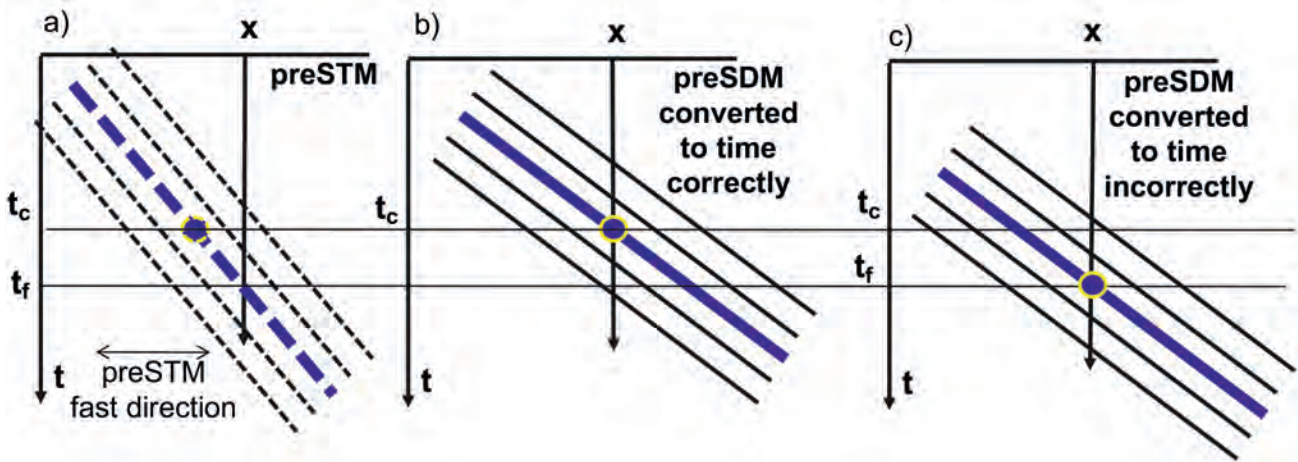


Figure 11 a) PreSTM, with marker image at time t_c , but with expected lateral mispositioning (repeat of image 10b). b) PreSDM converted to time correctly using the vertical component of the phase velocity, with marker appearing at time t_c . c) PreSDM converted to time so as to match the time-migration apparent well-tie time to the blue horizon at time t_f ; this is incorrect but 'looks right'.

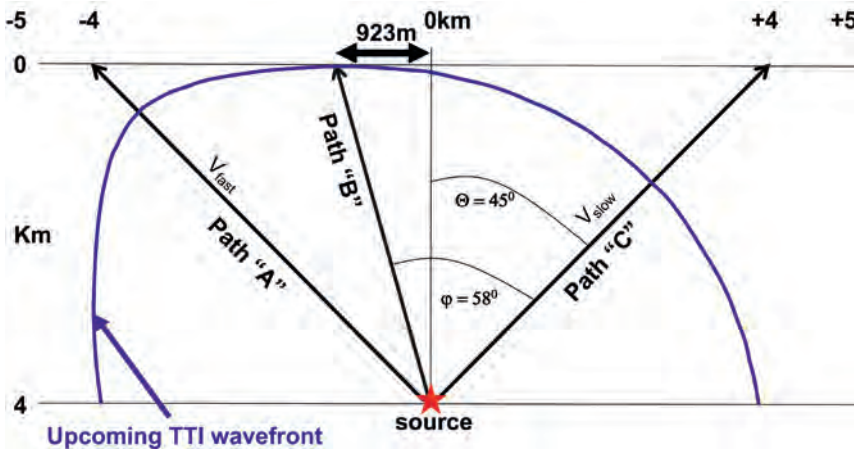


Figure 12 Homogeneous TTI anisotropic velocity model: polar axis tilt = 45° , $v_0 = 2000$ m/s, $V_{fast} = 2600$ m/s, $\epsilon = 0.3$, $\delta = 0.1$, with a buried source at 4km depth, under a split spread receiver array 10km wide. The arrival times for the receivers at ± 4 km are shown, corresponding to the slow and fast directions, respectively. Path A: path length=5.656 km, speed = 2600 m/s, $t = 2.175$ s. Path B: first arrival; path length = 4.1 km, angle = 58° , group velocity = 2280 m/s, $t = 1.818$ s. Path C: path length = 5.656 km, speed = 2000 m/s, $t = 2.828$ s. The expanding tilted anisotropic wavefront is shown (blue curve) just as it reaches the surface, giving rise to the first arrival time of 1.8 s. Plotted with true aspect ratio.

hence the horizontal direction must have a lower sound speed. However, the anisotropic preSTM implicitly assumes that the polar axis is vertical, hence it migrates the data with a higher lateral velocity than it should, moving the image sideways and additionally over-steepening the structure producing the expected preSTM lateral mispositioning (the dashed line structures shown in Figure 10b). At location 'x' in the preSTM, the vertical location of the dipping reflector appears to be at incorrect time t_f .

There are two components to this lateral preSTM displacement: firstly we have the 'side-slip' (e.g. Vestrum et al., 1999) which is the lateral shift between the correct TTI preSDM position and a false isotropic preSDM position (for this example, 545 m), and secondly, the component of lateral mispositioning occurring between isotropic preSTM and isotropic preSDM.

Converting the TTI preSDM to time with the vertical component of the phase velocity will move the blue dot at depth z_c in the preSDM to the same time as seen in the preSTM, namely t_c as shown in Figure 11b. However, this simple vertical stretch of the depth image cannot match the incorrect lateral shift of the preSTM image (Figure 11a). Now consider the scenario where the vertical black line at location x represents a well that penetrates the blue horizon. In the preSTM result (Figure 11a), the well intersects the blue horizon at false time t_f . Converting the preSDM to time with the (correct) vertical component of the phase velocity looks like a

mismatch at the well when comparing the blue horizon positions for the preSTM and time-converted depth images (Figure 11b), hence the temptation is to convert the preSDM to time with an incorrect lower velocity in order to match the well horizon-marker times by pushing down the time-converted preSDM from the correct time t_c to the greater time t_f (Figure 11c). In other words, we are trying to make a 'right' from two 'wrongs': time migration is always wrong and it cannot be made 'right' with a simple vertical stretch. Unfortunately, our two wrongs can only make another (and misleading) wrong. If we vertically stretched the preSDM to match the preSTM well-tie apparent time t_f , then any neighbouring flat events would no longer tie.

Converting a TTI preSDM to time to match direct measurements such as check-shots

In most of the discussion so far, we have dealt with *reflections*, which are composed of the coalescence of wavefronts, and hence arrive at the *phase* velocity. However, as noted with the *direct* wave arrivals, energy that travels *directly* from the source to a detector is travelling at the group velocity. Likewise, if we have to make comparisons with check shot data, the group velocity must be employed in conversions.

Figure 12 shows the exploding reflector modelling design of a buried source in a homogeneous anisotropic medium (as before

$v_0 = 2000$ m/s, $\delta = 10\%$, $\varepsilon = 30\%$, Polar dip = 45°). The source is at 4 km depth, so that the arrival time is comparable to the other modelling results (which had two-way arrival times of ~ 2 s), albeit here, it is a one-way travel time. The blue curve represents the expanding tilted anisotropic wavefront just as it reaches the surface, indicating where the first arrival will be seen on the receiver array. Figure 13 shows the associated split-spread shot record for the buried source, with various arrival times indicated. As this represents direct one-way arrivals, it is the group velocity which determines the arrival times from the buried scatterer to the surface.

However, if we did not know the location of the scatterer, we could not in practice make a point-to-point measurement. So knowing, say from borehole measurements, that the source was situated somewhere on a flat-lying reflector at 4km depth, and looking at a zero-offset seismic section, we would (erroneously) conclude that as the event arrived with one-way travel time of 1.818 s from a depth of 4 km, the upcoming plane wave must have travelled at a speed of 2222 m/s. This misconception arises as we would nominally assume that for the flat-lying reflector at 4 km depth, the zero-offset data would be recording the normal incidence arrivals. However, for an anisotropic medium, the zero offset incidence angle is not 90° . In other words, we have ignored the anisotropy side-slip component. If we knew the true subsurface location of the scatterer, as we might if it was a feature in a preSDM image, then we could use the side-slip to verify the correct distance travelled (which would be 4.1 km at the group velocity for this direction, namely 2280 m/s).

Conversion of a time image to geological depth for interpretation

Regardless of whether a time image was the result of a depth-migration (converted to time) or a direct time-migration, there will be circumstances when the check-shot velocity and/or unsmoothed group velocity should be used.

Such instances would be the cases where we want to compare the image to check-shot times or to compare interval-time maps

to those from previous time migrated data. However, if we wanted to compare horizon interval times of the high velocity layer with those from a previous time migration, we should not perform the conversion with a smooth model.

If the objective is to compare seismic horizons with check-shot information, then we need to be careful. Usually well ties would be done with depth domain data, so a problem does not arise, but if the interpreter wants to compare check-shot times with the time converted preSDM image, then converting to time with a smoothed model will probably introduce a mis-tie error. Performing a depth-to-time conversion with a detailed model might indeed give lateral distortions in the time image, but the check-shot mis-tie error from these distortions may be more acceptable to the interpreter than the image distortion associated with a rapidly changing velocity structure.

Comparison with vintage time images might also be easier if the depth to time conversion was performed with the actual preSDM model, and in addition, if we intend to perform several trial time to depth conversions with differing $v(z)$ functions, then the initial conversion from depth to time should be done with the actual preSDM model.

Conclusions

In the first part of this tutorial (Jones 2009), it was noted that on balance if we intend to apply post-migration pre-stack processing to preSDM data, it is preferable to time-convert the depth data using a smooth velocity model. In general this will not be the preSDM model itself, as this tends to include sharp velocity boundaries. Hence we need to introduce a new, separate velocity field for the purpose of depth-to-time conversion. If, however, the objective is to solely compare to check shot times, or horizon interval times, or to perform a suite of trial time-to-depth conversions, then the depth image could be time-converted with the actual preSDM model.

In this tutorial, I have extended the analysis to the case of anisotropic migration, and to describe the correct way of doing something inherently incorrect. In the presence of lateral

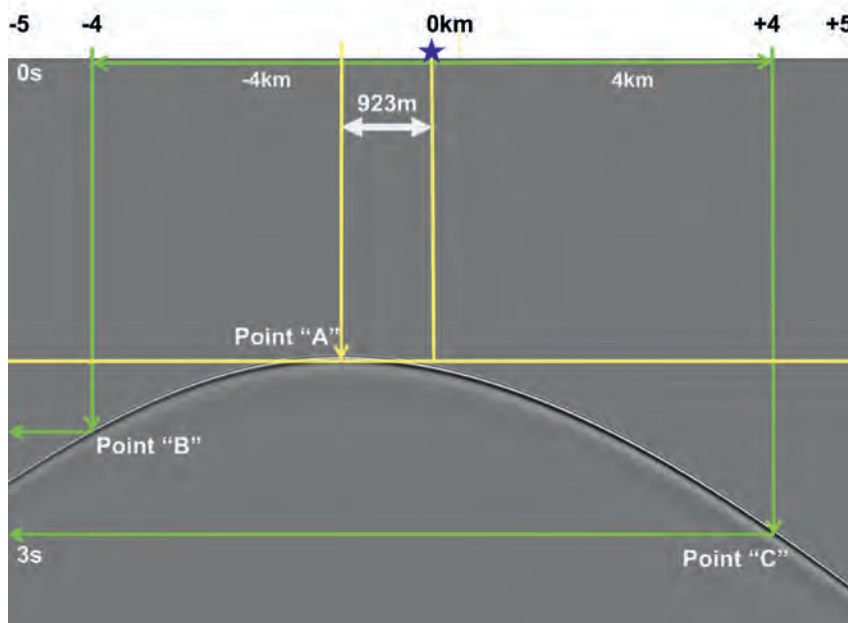


Figure 13 Seismic diffraction response of a scatterer at 4km depth beneath the centre of a 10km surface receiver spread (blue star), emulated with a buried source forward modelling exercise. The first arrival (point A) arriving at the group velocity of 2280 m/s, is at $t = 1.818$ s, shifted laterally from the scatterer location by 923 m (the anisotropic 'side-slip'). Arrival times for the events at ± 4 km are also shown: point B with path length = 5.656 km, speed = 2600 m/s, $t = 2.175$ s; point C with path length = 5.656 km, speed = 2000 m/s, $t = 2.828$ s.

heterogeneity on a scale length comparable to the migration aperture (several kilometres), a time migration does not relocate recorded energy to its correct spatial location, whereas a depth migration should do. Consequently, the notion of converting a depth image to the time domain via a vertical stretch, and then comparing it to a time migration is at best a dubious procedure. However, given that we are regularly required to make such comparisons, it is instructive to perform the conversions with the most appropriate velocity. However, if doing so, we should not expect adjacent structures with different dips to be equally comparable, as two or more ‘wrongs’ don’t make a ‘right’.

The errors committed in performing depth to time conversion for TTI preSDM data are relatively small when comparing results obtained with conversions performed with v_v or the vertical components of both group and phase velocity. For example, on some steeply dipping (60°) West African offshore shale diaper data, with an average sediment velocity of about 2000 m/s, the time difference in such conversions at a depth of 3 km was about 40 ms. However, it is instructive to understand that the correct approach is to use the vertical component of the phase velocity. Conversely, if comparing to point-to-point measurements, such as direct arrivals, check-shot data, or diffraction responses from a known location, the group velocity for the appropriate direction should be used. This will be the case if our objective is to convert to ‘geological’ depth via calibration with check-shot data. Also, as noted in the earlier depth-to-time conversion tutorial (Jones, 2009), a laterally smooth velocity field is preferred if our intention is to perform additional multichannel processing (such as noise suppression) or horizon autopicking.

Whatever our objective in performing these procedures, perhaps the thing to bear in-mind is that any comparisons we make will only be at best locally valid, and the velocity required for the ‘best’ comparison will vary from structure to structure: caveat emptor!

Acknowledgements

I would like to thank Marcin Kobylarski for producing the synthetic examples and Joe Zhou for helpful discussions, and Nick Bernitsas, John Brittan, and Jacques Leveille, Peter Rowbotham, and the *First Break* reviewers for their helpful suggestions in preparing the manuscript.

References

Al-Chalabi, M. [1974]. An analysis of stacking RMS average and interval velocities over a horizontally layered ground. *Geophysical Prospecting*, **22** (3), 458-475.

Al-Chalabi, M. [1994]. Seismic velocities—a critique. *First Break*, **12**, 589-596.

Al-Chalabi, M. [1997]. Parameter nonuniqueness in velocity versus depth functions. *Geophysics*, **62** (3), 970-979.

Al-Chalabi, M. and Rosenkranz, P.L. [2002]. Velocity-depth and time-depth relationships for a decompacted uplifted unit. *Geophysical Prospecting*, **50** (6), 661-664.

Al-Chalabi, M., [2014]. *Principles of Seismic Velocities and Time-to-Depth Conversion*. EAGE, Houten, The Netherlands.

Alkhalifah, T. and Larner, K. [1994]. Migration error in transversely isotropic media. *Geophysics*, **59** (9), 1405-1418.

Alkhalifah, T. and Tsvankin, I. [1995]. Velocity analysis for transversely isotropic media. *Geophysics*, **60** (5), 1550-1566.

Alkhalifah, T. [1997]. Velocity analysis using nonhyperbolic moveout in transversely isotropic media. *Geophysics*, **62** (6), 1839-1854.

Alkhalifah, T. [2000]. An acoustic wave equation for anisotropic media. *Geophysics*, **65**, 1239-1250.

Armstrong, T., [2001]. Velocity anomalies and depth conversion – drilling success on Nelson Field, Central North Sea. *63rd EAGE Conference & Exhibition*, Extended Abstracts, IV-2.

Armstrong, T.L., J. McAteer, and P. Connolly, [2001]. Removal of overburden velocity anomaly effects for depth conversion. *Geophysical Prospecting*, **49**, 79-99.

Bakulin, A., Woodward, M., Nichols, D., Osypov, K., and Zdraveva, O., [2010]. Building tilted transversely isotropic depth models using localized anisotropic tomography with well information. *Geophysics*, **75** (4), D27-D36.

Bale, R. [2007]. Phase-Shift Migration and the Anisotropic Acoustic Wave Equation. *EAGE 69th Conference & Exhibition*, Expanded Abstracts.

Bartel, D.C., Busby, M., Nealon, J., and Zaske, J., [2006]. Time to depth conversion and uncertainty assessment using average velocity modeling. *SEG*, Expanded Abstracts, **25**, 2166.

Berryman, J.G., [1979]. Long-wave elastic anisotropy in transversely isotropic media. *Geophysics*, **44** (5), 896-917.

Black, J.L. and Brzostowski, M.A. [1994]. Systematics of time migration errors. *Geophysics*, **59** (9), 1419-1434.

Cameron, M., Fomel, S., and Sethian, J., [2008]. Time-to-depth conversion and seismic velocity estimation using time-migration velocity. *Geophysics*, **73**, VE205.

Grechka, V. [2009]. *Applications of Seismic Anisotropy in the Oil and Gas Industry*. EAGE, Houten, The Netherlands.

Grechka, V., I. Tsvankin, and J. K. Cohen, [1999]. Generalized Dix equation and analytic treatment of normal-moveout velocity for anisotropic media: *Geophysical Prospecting*, **47**, 117-148.

Hubral, P. [1977]. Time migration; some ray theoretical aspects. *Geophysical Prospecting*, **25** (4), 738-745.

Iversen, E., and Tygel, M., [2008]. Image-ray tracing for joint 3D seismic velocity estimation and time-to-depth conversion. *Geophysics*, **73**, S99.

Jones, I.F., Bridson, M.L. and Bernitsas, N.X. [2003]. Anisotropic Ambiguities in TI Media. *First Break*, **21** (4), 31-37.

Jones, I.F. [2009]. Tutorial: Time conversion of depth migrated data. *First Break*, **27** (7), 51-55.

Jones, I.F. [2010]. *An introduction to velocity model building*. EAGE, Houten, The Netherlands.

Jones, I.F. and Davison, I. [2014]. Seismic imaging in and around salt bodies. *SEG Interpretation*, **2** (4), SL1-SL20.

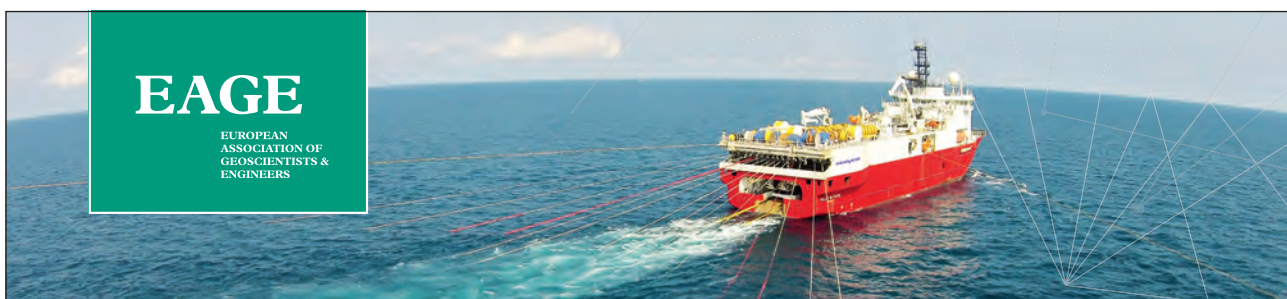
Jones, I.F. [2015]. Estimating subsurface parameter fields for seismic migration: velocity model building. In: Grechka, V. and Wapenaar, K. (Eds.), *Encyclopedia of Exploration Geophysics*. SEG, Tulsa, USA.

Robein, E. [2003]. *Velocities, time-imaging and depth-imaging: Principles and methods*. EAGE, Houten, The Netherlands.

Robein, E., [2010]. *Seismic Imaging: A Review of the Techniques, their Principles, Merits and Limitations*. EAGE, Houten, The Netherlands.

- Sadri, M. and Riahi, M.A. [2010]. Ray tracing and amplitude calculation in anisotropic layered media. *Geophys. J. Int.*, **180**, 1170-1180.
- Sugrue, M., Osolo, C., Anstey, I., Oladeji, O., and Gere, C. [2011]. TTI Depth Migration – Advantages for Development Offshore Nigeria. *81st Annual International Meeting*, SEG.
- Thomsen, L. [1986]. Weak elastic anisotropy. *Geophysics*, **51** (10), 1954-1966.
- Thomsen, L. [2002]. *Understanding seismic anisotropy in exploration and exploitation*. SEG/EAGE DISC course lecture notes.
- Tsvankin, I. and Thomsen, L. [1994]. Nonhyperbolic reflection moveout in anisotropic media. *Geophysics*, **59** (8), 1290-1304.
- Tsvankin, I. [1997]. Moveout analysis for transversely isotropic media with a tilted symmetry axis. *Geophys. Prosp.*, **45**, 479–512.
- Uren, N.F., Gardner, G.H.F. and McDonald, J.A. [1990]. Normal moveout in anisotropic media. *Geophysics*, **55** (12), 1634-1636.
- Vernik, L. and Liu, X. [1997]. Velocity anisotropy in shales: A petrophysical study. *Geophysics*, **62**, 521-532.
- Vestrum, R.W., Lawton, D.L. and Schmid, R. [1999]. Imaging structures below dipping TI media. *Geophysics*, **64** (4), 1239-1246.
- VerWest, B.J. [1989]. Seismic migration in elliptically anisotropic media. *Geophysical Prospecting*, **37** (2), 149-166.
- Wang Y. [2014]. Seismic ray tracing in anisotropic media: A modified Newton algorithm for solving highly nonlinear systems. *Geophysics*, **79**, T1-T7.

ADVERTISEMENT



Second EAGE Marine Acquisition Workshop

25-27 AUGUST 2020 • OSLO, NORWAY

• **Submit your Abstract!**

WWW.EAGE.ORG

